



Year: 2019

Accuracy of an automated three-dimensional technique for the computation of femoral angles in dogs

Longo, Federico ; Savio, Gianpaolo ; Contiero, Barbara ; Meneghello, Roberto ; Concheri, Gianmaria ; Franchini, Federico ; Isola, Maurizio

Abstract: **Aims:** The purpose of the study was to evaluate the accuracy of a three-dimensional (3D) automated technique (computer-aided design (aCAD)) for the measurement of three canine femoral angles: anatomical lateral distal femoral angle (aLDFA), femoral neck angle (FNA) and femoral torsion angle. **Methods:** Twenty-eight femurs equally divided into two groups (normal and abnormal) were obtained from 14 dogs of different conformations (dolichomorphic and chondrodystrophic). CT scans and 3D scanner acquisitions were used to create stereolithographic (STL) files, which were run in a CAD platform. Two blinded observers separately performed the measurements using the STL obtained from CT scans (CT aCAD) and 3D scanner (3D aCAD), which was considered the gold standard method. Correlation coefficients were used to investigate the strength of the relationship between the two measurements. **Results:** The accuracy of the aCAD computation was good, being always above the threshold of $R > 0.8$ for all three angles assessed in both groups. aLDFA and FNA were the most accurate angles (accuracy $> 90\%$). **Conclusions:** The proposed 3D aCAD protocol can be considered a reliable technique to assess femoral angle measurements in canine femur. The developed algorithm automatically calculates the femoral angles in 3D, thus considering the subjective intrinsic femur morphology. The main benefit relies on a fast user-independent computation, which avoids user-related measurement variability. The accuracy of 3D details may be helpful for patellar luxation and femoral bone deformity correction, as well as for the design of patient-specific, custom-made hip prosthesis implants.

DOI: <https://doi.org/10.1136/vr.105326>

Posted at the Zurich Open Repository and Archive, University of Zurich

ZORA URL: <https://doi.org/10.5167/uzh-172071>

Journal Article

Accepted Version

Originally published at:

Longo, Federico; Savio, Gianpaolo; Contiero, Barbara; Meneghello, Roberto; Concheri, Gianmaria; Franchini, Federico; Isola, Maurizio (2019). Accuracy of an automated three-dimensional technique for the computation of femoral angles in dogs. *Veterinary Record*, 185(14):443.

DOI: <https://doi.org/10.1136/vr.105326>

1 **Research article**

2

3

4 **Accuracy of an automated three-dimensional technique for the**
5 **computation of femoral angles in dogs**

6

7

8 F. Longo ^{a,d*}, G. Savio ^b, B. Contiero ^a, R. Meneghello ^c, G. Concheri ^b, F. Franchini^b, M. Isola ^a

9

10 ^a *Department of Animal Medicine, Production and Health, University of Veterinary Medicine,*
11 *Padova, Italy*

12 ^b *Laboratory of Design Tools and Methods in Industrial Engineering, Department of Civil,*
13 *Architectural and Environmental Engineering, University of Engineering, Padova, Italy*

14 ^c *Department of Management and Engineering, University of Padova, Vicenza, Italy*

15 ^d *Clinic for Small Animal Surgery, Vetsuisse Faculty University of Zurich, Zurich, Switzerland*

16

17

18

19

20

21

22 * Corresponding author. Tel: +39 049 8272608.

23 *E-mail address: flongo@vetclinics.uzh.ch (F. Longo).*

24

25

26

27

28

29

30

31

32

33

34

35 **Abstract**

36 The purpose of the study was the evaluation of the accuracy of a three-dimensional (3D) automated
37 technique (aCAD) for the measurement of three canine femoral angles: anatomical lateral distal
38 femoral angle (aLDFA); femoral neck angle (FNA); and femoral torsion angle (FTA).

39 Twenty-eight femurs equally divided in 2 groups (normal and abnormal) were obtained from 14
40 dogs of different conformations (dolichomorphic and chondrodystrophic).

41 Computed tomographic (CT)-scans and 3D scanner acquisitions were used to create
42 stereolithographic (STL) files which were run in a computer-aided-design (CAD) platform. Two
43 blinded observers performed separately the measurements using the STL obtained from CT-scans
44 (CT aCAD) and 3D scanner (3D aCAD), which was considered the gold standard method.

45 The correlation coefficients were used to investigate the strength of the relationship between the
46 two measurements.

47 The accuracy for the aCAD computation was good, being always above the threshold of $R^2 > 80\%$
48 for all three angles assessed in both groups. ALDFA and FNA were most accurate angles (accuracy
49 $> 90\%$).

50 The proposed 3D aCAD protocol can be considered a reliable technique to assess femoral angle
51 measurements in the canine femur. The developed algorithm automatically calculates the femoral
52 angles in 3D, thus considering the subjective intrinsic femur morphology. The main benefit relies
53 on a fast user-independent computation, which avoid user-related measurement variability. The
54 accuracy of 3D details may be helpful for patellar luxation and femoral bone deformity correction
55 as well as for the design of patient specific custom-made hip prosthesis implants.

56
57 *Keywords:* Accuracy, Dog; Femur; Computed tomography; Three-dimensional constructions; 3D
58 scanner

59 **Introduction**

60
61 The state of art for the measurement of angles in the canine femur has been traditionally limited to
62 multiple orthogonal radiographs (RX),¹⁻³ which were gradually overtaken by the computed
63 tomography (CT)-scans^{4,5} and magnetic resonance (MRI) evaluations.^{6,7} These latter two
64 diagnostic techniques exhibit satisfactory aptitudes in terms of bone and images manipulation,
65 avoiding the positioning issue that frequently characterizes the radiographic evaluation.^{4,8} However,
66 CT and MRI lack on real three-dimensional (3D) measurement of angles since that almost for all
67 the values proposed by the literature were achieved with two-dimensional (2D) imaging.^{6,9,10}
68 Recently a 3D Python-based algorithm run on a computer-aided-design (CAD) software
69 (Rhinoceros version 5, Robert McNeell & Associates) was presented as a novel methodology for
70 the computation of femoral angles in the canine femur.^{11,12} The femoral angles computed,
71 differently from those obtained using different diagnostic techniques,¹⁻¹⁰ were measured in a real
72 3D fashion. The main benefit relies on automated measurements, which are independent from the
73 points selected by the operator, bone orientation and conformation as well. As a result, the operator-
74 related measurement variability is decreased as the manual manipulation of the bone model and the
75 identification of target anatomical landmarks are not required. The repeatability and reproducibility
76 of the proposed protocol were assessed and compared with manual measurements made with
77 radiographs and CT reconstructions, finding that the 3D protocol was the most repeatable and
78 reproducible method.¹² This conclusion was, also, supported by the automated design of the 3D
79 protocol, which restricts the potential user-related errors only to the operations required for the
80 creation of the mesh model and, therefore, remarkably decreases the computational time.¹¹
81 However, the accuracy of 3D measurements, described as the difference of a measured value from a
82 true value, was not assessed and needed to be investigated. Therefore, the purpose of this study was
83 to determine the accuracy of our aCAD protocol for the computation of three femoral angles in

84 dogs: anatomical lateral distal femoral angle (aLDFA); femoral neck angle (FNA); and femoral
85 torsion angle (FTA).

86 Polygonal mesh models were created from 3D reconstructions of CT images and femoral angles
87 were computed with the developed protocol. The values obtained were compared to the
88 measurements performed with the same aCAD protocol but executed on polygonal mesh models
89 generated by 3D scans, which due to its high-resolution 3D nature, was assumed as the gold
90 standard technique for this study.

91 The second object of this study was to assess the efficacy of the aCAD protocol for the
92 measurement of femoral angles in either normal or abnormal femurs.

93

94

95

96

97

98

99

100

101

102

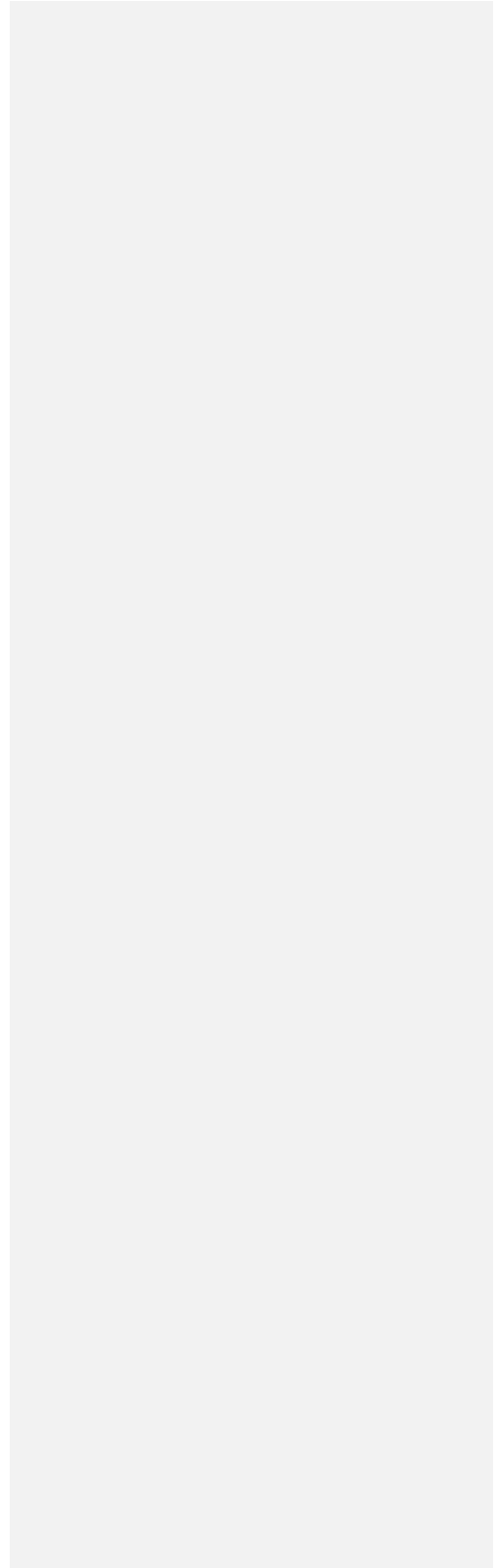
103

104

105

106

107



108

109

110

111 **Materials & Methods**

112

113 Fourteen canine paired pelvic limbs were collected. The cadavers were euthanized for reasons
114 unrelated with this project and a signed informed consent was requested before proceeding with
115 imaging acquisition and femur disarticulation. The study was conducted in a double-blind fashion
116 by two observers (an orthopaedic surgeon and an engineer). Moreover, one experienced radiologist
117 acquired all radiographic and CT images. He, also, anonymised all CT scans using a legend and
118 separately packed every femur sample to prevent any conditioning for the observers.

119 Specimens were first radiographed with digital radiographic equipment (Kodak Point of Care CR-
120 360 System, Carestream Health). A standard ventro-dorsal and latero-lateral views were performed.

121

122 *CT scans*

123 CT scans were then acquired with four multi-detector row CT scanner (Toshiba Asteion S4,
124 Toshiba Medical Systems Europe). Dogs were positioned with a supine recumbence with legs
125 adducted, extended and tied above the stifles. An amperage of 150 mA, exposure time of 0.725 s
126 and voltage of 120 kV were set on. A slice thickness of 1 mm (reconstruction interval 0.8 mm) was
127 applied. CT images were reconstructed with a high-resolution filter for bones with the following
128 bone window (window length 1000 Hounsfield units, HU; window width 4000 HU). A 3D volume
129 reconstruction was done using a DICOM-processing software (Osirix version 2.7, pixmeo SARL).
130 The first observer isolated with Osirix every anonymized femur by cropping the tibia and pelvis,
131 avoiding unintentional modification of the profiles of the femoral head and condyles. Once the
132 femur model was separated, it was segmented using the procedure described by Longo et al.¹²
133 Briefly, using the region of interest (ROI) and 2D/3D growing region software functions, the

134 observer found the mean density femur values, which usually are major than 300 Hounsfield unit
135 (HU) and then set-up the segmentation parameters in a dedicated tool window. As a result, a
136 bitmapped (newly generated imaging series) was created and 3D reconstructed, through surface
137 rendering function. Finally, a 3D stereolithographic (STL)¹³ file was saved and imported in the
138 Rhinoceros platform.^{11,12}

139

140 *3D scans*

141 STL files were generated from 3D scans to obtain reference models on which compare femoral
142 angles measured on CT. Femurs were disarticulated at coxo-femoral and femoral-tibial joints,
143 dissected free from soft tissues excluding the patella and fabellae and stored in plastic bags at a -
144 20°. A 3D scanner (Cronos 3D dual, Open technologies) was used for the femoral analysis. The
145 second observer positioned every anonymised femur on a circular rotating platform. The scanning
146 of the femur was performed adopting a triangulation technique, based on cameras, characterized by
147 a predetermined convergence angle and a fringe projector. The platform was automatically rotated
148 of a predetermined angle sequence, obtaining at least 5 to 10 acquisitions. A 3D geometrical bone
149 model was generated superimposing and aligning the multiple views of the model, obtained per
150 each sequence, by means of an engineering software (Optical RevEng, Open technologies).
151 Cleaning, filtering and closing-holes phases were used to delete model inaccuracies such as noises
152 and local spikes. As a result, a high-resolution mesh model of the bone was obtained and saved as a
153 STL file. The accuracy of the 3D scanner is $\pm 30 \mu\text{m}$.¹⁴ Similar results were obtained by the internal
154 verification procedure based on ISO (10360-8:2013) at the Laboratory of Design Tools and
155 Methods in Industrial Engineering. Considering that the 3D scanner accuracy is higher more than an
156 order of magnitude compared to CT axial resolution (0.8 mm), it is possible to assume the 3D scan
157 models as reference.

158

159

160

161

162 *Automated-CAD measurements from CT reconstructions (CT aCAD) and 3D scanner*
163 *(3D aCAD)*

164 Both observers imported each CT (Fig. 1) or 3D (Fig. 2) STL file in the CAD software where the
165 aCAD protocol was used to measure femoral angles. The aCAD computation was performed
166 following the same procedure steps described by Savio et al.¹¹ In brief, the vertices inside the
167 femoral medullary canal (internal mesh) were selected and deleted. This operation is needed to
168 improve the quality of axis drawing and angle measurements, as the presence of internal vertices
169 may interfere with the automatic computation. Then, the femoral analysis was initiated by clicking
170 on the femoral head. To compute the femoral angles, the developed algorithm first identifies points,
171 planes and axis into the femur mesh. It performed all the measurements in few minutes through four
172 automatic phases: 1) femur alignment; 2) proximal femoral long axis computation; 3) analysis of
173 the proximal femoral epiphysis; 4) analysis of the distal femoral epiphysis. During these two final
174 phases, the vertices representing the femoral head and condyles were superimposed by spheres (Fig.
175 1 and 2).^{11,12} Finally, aLDFA, FNA and FTA angles were displayed on the screen and recorded by
176 the observer.

177

178 *Groups*

179 Considering radiographic, CT and visual gross evaluation, the specimens were examined for
180 evidence of osteoarthritis (OA) and difference of breed conformation (dolichomorphic vs
181 chondrodystrophic). The femurs were divided in two groups. Group 1 was assigned as normal,
182 adopting the following inclusion criteria: femurs were obtained from dolichomorphic breeds with no
183 evidence of OA. Whereas the second category was more heterogenic and included femurs either
184 affected by OA regardless of conformation or taken from chondrodystrophic breeds (Fig. 3).

185 The radiologist radiographically evaluated the degree of OA and converted the OA score to a
186 numeric scale (0= none; 1= mild; 2= moderate ;3= severe).^{15,16}

187

188

189 *Statistical analysis*

190 The statistical analyses were performed using a commercially available software (SAS 9.4, SAS
191 Institute Inc., Cary, NC, USA). Normality distribution hypothesis was assessed by Shapiro-Wilk
192 test. A linear regression analysis was applied, considering the gold standard method (3D aCAD) as
193 the independent variable and the CT aCAD as the dependent variable.

194 The adjusted R² was used to quantify the strength of the relationship between the angle measured
195 through CT aCAD (observer 1) and 3D aCAD (observer 2) techniques. Adjusted R² values > 80 %
196 were considered acceptable. The hypotheses of the linear model on the residuals were graphically
197 assessed.

198 The descriptive statistics (means, standard deviations, medians and interquartile ranges) were
199 calculated for each angle (aLDFA, FNA and FTA) measurements for both imaging techniques.

200 The paired Student t-test was performed to compare the data recorded with CT aCAD and the gold
201 standard. Statistical significance of P-value was set at < 0.05.

202

203

204

205

206

207

208

209

210

211

212
213
214
215
216
217
218

Results

219 Twenty-eight femurs divided in two groups (1 = normal, 2= abnormal) of 14 femurs each, were
220 used for this study. The specimens were obtained from dogs of different breeds and conformations:
221 3 mixbreed dogs, 2 Dachshunds, 2 French bouledogs and 1 Pug, German shepherd, Labrador R.,
222 Bernese mountain dog, Segugio italiano, Amstaff and Great Dane. Ten dogs were intact males, 3
223 were spayed females and 1 was a not-spayed female. The overall mean body weight was 19.5 kg
224 (range 4-44 kg), whereas the body weight means of the groups were: group 1 (16.1 kg, range 13-28
225 kg) group 2 (19.3 kg, range 4-44 kg). The overall mean age was 9.5 years (range 2-15 years). The
226 mean age of group 1 was 4.7 years (range 2-8 years), while group 2 had a mean age of 12.5 years
227 (range 9-15 years).

228 Group 1 included 14 dolicomorphic femurs with no evidence of radiographic OA. Within the 14
229 femurs of the group 2, there were: 4 chondrodystrophic femurs not affected by OA, 6
230 chondrodystrophic femurs affected by OA (mean OA score: 1) and 4 dolicomorphic femurs affected
231 by OA (mean OA score: 2).

232 All data regarding the 3 angles and for both CT aCAD and 3D aCAD measurements were normally
233 distributed (Shapiro-Wilk test >0.9). The values of the angles recorded were well aligned along
234 regression lines in almost all the samples, excepted for some femurs included in group 2 (Fig. 4)
235 The adjusted R² value of the CT aCAD and 3D aCAD measurements resulted always above the
236 acceptance criterion of 80%, regardless of the angle measured and the group considered. Overall,
237 the coefficients calculated for all 28 femurs were: aLDFA > 95%; FNA > 95% and FTA > 86%
238 (Fig. 4). Specifically, within group 1 the coefficients were: aLDFA > 93%; FNA > 93% and FTA >

239 98%, while within group 2: aLDFA > 97%; FNA > 94% and FTA > 82% (Fig. 4). Technique-
240 related means, medians and interquartile ranges values for the 3 angles are displayed in Table 1.
241 The t-test showed that there was not a statistically significant difference ($P < 0.05$) in the mean
242 difference values of each paired measurements for every angle assessed, excepted for FTA
243 measurement in group 2 (Table 2)

244 **Discussion**

245 This study investigated the accuracy of a novel automated 3D technique (aCAD) for the
246 computation of canine femoral angles. We used the correlation coefficients to assess the strength of
247 the relationship between the angle measurements performed by the observers in Rhino starting from
248 STL files created either from CT-scans (CT aCAD) or 3D scanner (3D aCAD). The aCAD
249 methodology has, looking at the accuracy investigation, been satisfactory for all three angles
250 assessed (> 82%).

252 This suggests that the CT aCAD measurements were comparable to the 3D aCAD measurements,
253 which represented our reference standard method of assessment. The practical consequence is that
254 the developed 3D protocol is not only repeatable and reproducible¹² but also may be considered
255 enough accurate. However, a validation of the 3D scanner on bone measurements needs to be
256 performed to corroborate this subjective assumption.

257 The accuracy of a test is a description of how close a measured value is to an assumed true value;
258 which means that a “true” value must be both identifiable and measurable, thus providing an
259 unequivocal gold standard against which new tests may be assessed.^{4,16} In this study, we have
260 assumed 3D scanner measurements of femoral anatomic specimens as the gold standard method for
261 two main reasons. First, 3D scanner allows for creating detailed and precise geometrical bony
262 models¹⁷ that could nicely reproduce the original femoral morphology. We have applied white spray
263 onto the femoral specimens and waited at least 24 hours before the image acquisition with the
264 scanner. The aim was to increase the visualization of the femoral cortices, decreasing the radio-

265 transparency of the bone and thus improve the quality of the femoral captures. Second, 3D scanner
266 allows the user to work with real 3D files, which we cannot obtain from other reported two-
267 dimensional techniques.^{9,18} It may be argued that we could have either measured the femoral angles
268 on digital photography images of femur specimens or calculated them directly onto the bones.
269 Although, the quantification of an established “true” value for a such variable measurement (angle)
270 depends on arbitrary anatomic landmarks, in the authors’ opinion a comparison between a 3D
271 technique (aCAD) with a 2D gold standard method (digital photography) wouldn’t be feasible. The
272 reason is attributable to the structured differences of the methodologies tested.
273 A direct measurement of femoral angles onto femurs specimens could have represented an
274 alternative gold standard. However, we believe that such method couldn’t represent an accurate
275 methodology as well because precise anatomic reference lines needed to be drawn, increasing the
276 risk of operator-measurement errors.
277 Overall, the aLDFA and FNA were the most accurate angles since that their correlation coefficients
278 were always above the 90% threshold, regardless of the groups considered. FTA measurements
279 were still satisfactory but showed a lesser accuracy. These results partially confirmed the data that
280 we previously presented.¹² Specifically, the aLDFA represents the most repeatable, reproducible
281 and accurate angle to measure. The FNA, which resulted as the lesser repeatable and reproducible
282 angle to be quantified with three different diagnostic techniques (RX, CT and aCAD computation),
283 here exhibited comparable values between CT aCAD and 3D aCAD. Whereas, the measurements
284 recorded for the FTA resulted as the most out of range from the real values, but still within the
285 established threshold of acceptance (> 80%) in both normal and abnormal femurs.
286 The computation ability of the developed protocol in femurs of different dimensions, conformations
287 (dolichomorphic and chondrodystrophic breeds) as well as in femurs affected or unaffected by OA,
288 represented a key point of our project. Previously, the described 3D protocol was performed mrely
289 on normal femurs, free of orthopaedic diseases.^{11,12}

290 The femoral angles measured by the observers are commonly quantified in the preoperative
291 planning of patellar luxation,^{5,19} which is frequently caused by femoral deformities.^{20,21} These
292 skeletal malformations cause imbalanced joint loading and when they are either severe or lately
293 diagnosed (chronic), they may lead to OA which deforms the articular profiles.²²⁻²⁴ In this study, 10
294 out of 28 femurs were affected by OA, of which one (femur 19) had a severely arthritic femoral
295 head (OA score: 3) (Fig. 5) and two (femurs 25 and 26) had the condylar profiles altered (OA score:
296 2). The massive remodeling of the articular profiles, above all of the femoral head, represents both a
297 challenge for the computational analysis and a plausible explanation for a less than perfect accuracy
298 detected for the FTA. The algorithm needs to correctly identify and fit the original sphere of the
299 femoral head and condyles. During the pilot developing phase, the algorithm was set up to exclude
300 from the analysis all the vertices that belong to external components of the femoral head fitting such
301 as osteophytes, which could potentially alter the computational analysis.¹¹ The FTA correlation
302 coefficient obtained for the computation of abnormal femurs ($R^2=82\%$) means that the algorithm
303 effectively analyses also deformed femoral heads but not as accurately as for FNA and aLDFA
304 computation ($\geq 92\%$). Considering the satisfactory FTA accuracy in the normal group (R^2 FTA >
305 98%), we attribute the lower FTA accuracy in abnormal femurs mainly to the difficulty of analysing
306 severely altered femoral head profiles. However, the accuracy obtained was still major than 80%
307 threshold ($R^2=82\%$).

308 The descriptive statistic displayed in Table 1 shows that the values measured for FNA and FTA fall
309 within the ranges described in the literature: FNA (125° - 138°)^{3,25} and FTA (12 - 40°).^{2, 25}

310 The FNA and especially FTA reference ranges are wide.^{2,3,25} In the authors' opinion this is
311 concerning and need to be clarified as femoral torsion is frequently detected in case of patellar
312 luxation and need to be often corrected. The accepted clinical tolerance for FTA suggests that there
313 is a variable either depending on the femur morphology or on the observer ability which influences
314 the angle measurements. Explanations may rely on the identification of the target points such as the
315 center of the femoral head and neck, which could be challenging for the observer, especially in the

316 case of severe OA. Our FTA mean ranges from 20-22° (table 1), which agrees with our previous
317 results^{11,12} and with the literature ranges.^{2,25} However, sometimes a 27° reference value for femoral
318 torsional deformity is assumed,²⁰ and therefore the obtained FTA mean implies that our 3D
319 technique identifies a more retroverted position of the femoral head. Whether this result may have a
320 clinical impact could not be answered with this study and therefore need to be further investigated.
321 The aLDFA mean values, accordingly with those already found by the authors^{11,12} are slightly
322 lower than the reported range (aLDFA 94-98°).^{3,25} We impute this result mainly to morphologic
323 heterogeneity of the femurs computed. We analyzed a range of femurs of different dimensions
324 (small to large dogs) and conformations (dolichomorphic and chondrodystrophic), while the data
325 reported in literature were obtain mainly in large dolichomorphic dogs.^{16,25} It is plausible to expect
326 that chondrodystrophic dogs as well as small size breeds may be characterized by different values
327 regarding frontal and torsional femoral alignment. Furthermore, the t-test analysis exhibited a not
328 significant difference for each paired of values assessed. In almost for all the cases evaluated, the
329 CT aCAD measurements tended towards underestimating the femoral angle values compared to the
330 gold standard, but this tendency was statistically significant only for the femoral torsion evaluation
331 in the group of abnormal femurs (Table 2).

332

333 **Conclusions**

334 We have shown that the automatic measurements obtained from CT derived data are
335 significantly comparable with high-resolution 3D scanner-derived data, suggesting that the tested
336 automated CAD technique is an accurate methodology for measuring femoral angles in both normal
337 and abnormal canine femurs. However, currently it is not validated what should a gold standard be
338 for 3D measurements. Therefore, further studies could be undertaken to compare anatomical versus
339 3D scanner measurements of bones.

340 The presented methodology could represent a reliable diagnostic method to adopt when a femoral
341 deformity is suspected, having the automated and 3D nature of its assessments and rapidity of its
342 computational analysis as main substantial benefits. Moreover, the precision of patellar luxation
343 planning may increase, due to the user-independent structure of measurements. Finally, the
344 possibility to correctly identify anatomic landmarks such as the original curvature of the femoral
345 head, the external and internal profiles of the femoral neck, and potentially the original morphology
346 of the acetabulum, even in the case of a severe degenerative joint disease, may extend its
347 usefulness in the future, also, for arthroplasty purposes. However, further evaluations need to be
348 done with a greater number of samples to improve the quality and the precision of the femur
349 computation in severely arthritic femoral heads.

350

351 **Conflict of interest statement**

352 None of the authors of this paper have a financial or personal relationship with other people
353 or organisations that could inappropriately influence or bias the content of the paper.

354

355

356

357

358

359

360

361

362

363

364

365

366

367

368
369
370
371
372
373
374
375
376
377
378
379
380
381
382
383
384
385
386
387
388
389
390
391
392
393
394
395
396
397
398
399
400
401
402
403
404
405
406
407

References

1. Bardet JF, Rudy RL, Hohn RB. Measurement of femoral torsion in dogs using a biplanar method. *Vet Surg* 1983;12:1-6.
2. Montavon, P.M., Hohn, R.B., Olmstead, M.L., Rudy, R.L., 1985. Inclination and anteversion angles of the femoral head and neck in the dog evaluation of a standard method of measurement. *Vet Surg* 1985;14:272-282.
3. Tomlison, J, Fox D, Cook JL, *et al.* Measurement of femoral angles in four dog breeds. *Vet Surg* 2007;36:593-598.
4. Oxley B, Gemmill TJ, Pink J, *et al.* Precision of a novel computed tomographic method for quantification of femoral varus in dogs and an assessment of the effect of femoral malpositioning. *Vet Surg* 2013;42:751-758.
5. Barnes, D.M., Anderson, A.A., Frost, et al. Repeatability and reproducibility of measurements of femoral and tibial alignment using computed tomography multiplanar reconstructions. *Vet Surg* 2015;44:85-93.
6. Kaiser S, Cornely D, Golder W, *et al.* The correlation of canine patellar luxation and the anteversion angle as measured using magnetic resonance images. *Vet Radiol Ultrasound* 2001;42:113-118.

hat formatiert: Deutsch (Schweiz)

- 408 7. Ginja MMD, Ferreira, AJA, Jesus SS, *et al.* Comparison of clinical, radiographic, computed
409 tomographic, and magnetic resonance imaging methods for early prediction of canine hip
410 laxity and dysplasia. *Veterinary Radiol Ultrasound* 2009;50:135-143.
411
- 412 8. Jackson GM, Wendelburg KL. Evaluation of the effect of distal femoral elevation on
413 radiographic measurement of the anatomic lateral distal femoral angle. *Vet Surg*
414 2012;41:994-1001.
415
- 416 9. Dudley RM, Kowaleski MP, Drost, WT, *et al.* Radiographic and computed
417 tomographic determination of femoral varus and torsion in the dog. *Veterinary Radiol*
418 *Ultrasound* 2006;47:546-552.
419
- 420 10. Yasukawa S, Edamura K, Tanegashima K, *et al.* Evaluation of bone deformities of the
421 femur, tibia, and patella in Toy Poodles with medial patellar luxation using computed
422 tomography. *Vet Comp Orthop Tramadol* 2016;29:29-38.
423
- 424 11. Savio G, Baroni T, Concheri G, *et al.* Computation of femoral canine morphometric
425 parameters in three-dimensional geometrical models. *Vet Surg* 2016;45:987-995.
426
- 427 12. Longo, F., Nicetto, T., Banzato T, *et al.* Automated computation of femoral angles in dogs
428 from three-dimensional computed tomography reconstructions: Comparison with manual
429 techniques. *Vet J* 2018;232:6-12.
430
- 431 13. Botsch M, Kobbelt L, Pauly M, *et al.* Mesh data structures. In: Botsch ed. *Polygon Mesh*
432 *Processing*, 1st Edn. MA, USA: A.K. Peters, 2010 pp. 21-28
433
- 434 14. [https://www.growshapes.com/store/p137/Open-Technologies-3D-Scanner/Cronos-3D-Dual-](https://www.growshapes.com/store/p137/Open-Technologies-3D-Scanner/Cronos-3D-Dual-3MP.html)
435 [3MP.html](https://www.growshapes.com/store/p137/Open-Technologies-3D-Scanner/Cronos-3D-Dual-3MP.html). Last access 12/04/2019.
436
- 437 15. Lopez MJ, Lewis BP, Swaab ME, *et al.* Relationships among measurements obtained by use
438 of computed tomography and radiography and scores of cartilage microdamage in hip joints
439 with moderate to severe joint laxity of adult dogs. *Am J Vet Res* 2008;69:362-370.
440
- 441 16. D'Amico LL, Xie L, Abell LK *et al.* Relationships of hip joint volume ratios with degrees of
442 joint laxity and degenerative disease from youth to maturity in a canine population
443 predisposed to hip joint osteoarthritis. *Am J Vet Res* 2011;72:376-383.
444
- 445 17. Palmer RH, Ikuta CL, Cadmus JM 2011. Comparison of femoral angulation measurement
446 between radiographs and anatomic specimens across a broad range of varus conformations.
447 *Vet Surg* 2011;40:1023-1028.
448
- 449 18. Fahrni S, Campana L, Dominguez A, *et al.* CT-scan vs. 3D surface scanning of a skull: first
450 considerations regarding reproducibility issues. *Forensic Sciences Research* 2017;2:99-99.
451
- 452 19. Swiderski JF, Radecki SV, Park RD, *et al.* Comparison of radiographic and anatomic
453 femoral varus angle measurements in normal dogs. *Vet Surg* 2008;37:43-48.
454
- 455 20. Gibbons SE, Macias C, Tonzing MA, *et al.* Patellar luxation in 70 large breed dogs. *J Small*
456 *Anim Pract* 2006; 47: 3-9.
457

hat formatiert: Deutsch (Schweiz)

hat formatiert: Deutsch (Schweiz)

hat formatiert: Deutsch (Schweiz)

hat formatiert: Deutsch (Schweiz)

- 458 21. Brower BE, Kowaleski MP, Peruski AM, *et al.* Distal femoral lateral closing wedge
 459 osteotomy as a component of comprehensive treatment of medial patellar luxation and
 460 distal femoral varus in dogs. *Vet Comp Orthop Tramadol* 2017;20-27.
 461
 462 22. Roch SP, Gemmill TJ. 2008. Treatment of medial patellar luxation by femoral closing
 463 wedge osteotomy using a distal femoral plate in four dogs. *J Small Anim Pract*
 464 2008;249:52–158.
 465
 466 23. Dobbe J, du Pre` KJ, Kloen P, *et al.* Computer-assisted and patient-specific 3-D planning
 467 and evaluation of a single-cut rotational osteotomy for complex long-bone deformity.
 468 *Medical & Biological Engineering & Computing* 2011;49:1363–1370.
 469
 470 24. Milner SA, Davis TR, Muir KR, *et al.* Long-term outcome after tibial shaft fracture: is
 471 malunion important? *Journal of Bone and Joint Surgery American volume* 2002; 84A:971–
 472 980.
 473
 474 25. Petazzoni, M. Radiographic measurements of the femur. In: Petazzoni, M., Jaeger, G.H.
 475 (Eds). *Atlas of Clinical Goniometry and Radiographic Measurements of the Canine Pelvic*
 476 *Limb. 2nd Edn. Merial, Milano, Italy: Merial, 2008, pp. 34-54.*
 477
 478
 479
 480
 481
 482
 483

hat formatiert: Deutsch (Schweiz)

hat formatiert: Deutsch (Schweiz)

hat formatiert: Deutsch (Schweiz)

484
 485 Table 1 descriptive statistics measured with both computed tomography (CT aCAD: tested
 486 protocol) and 3D scanner (3D aCAD: gold standard) techniques for each angle.
 487

Technique		aLDFA	FNA	FTA
CT aCAD	Mean ± SD	92.51 ± 5.4	125.32 ± 10.2	21.96 ± 7.1
	Median	92.7	127.96	21.58
	IQR	7.7	8.28	8.8
3D aCAD	Mean ± SD	92.55 ± 5.3	124.26 ± 10.8	20.87 ± 6.4
	Median	92.2	126.8	20.2
	IQR	6.95	11.85	6.25

488
 489 Table 2 Mean difference and P-value of paired t-test calculated for each angle.

T- test	aLDFA		FNA		FTA	
	Normal	Abnormal	Normal	Abnormal	Normal	Abnormal
Mean	- 0,14°	0,22°	- 0.24	- 0.24	- 0.41	- 1.77

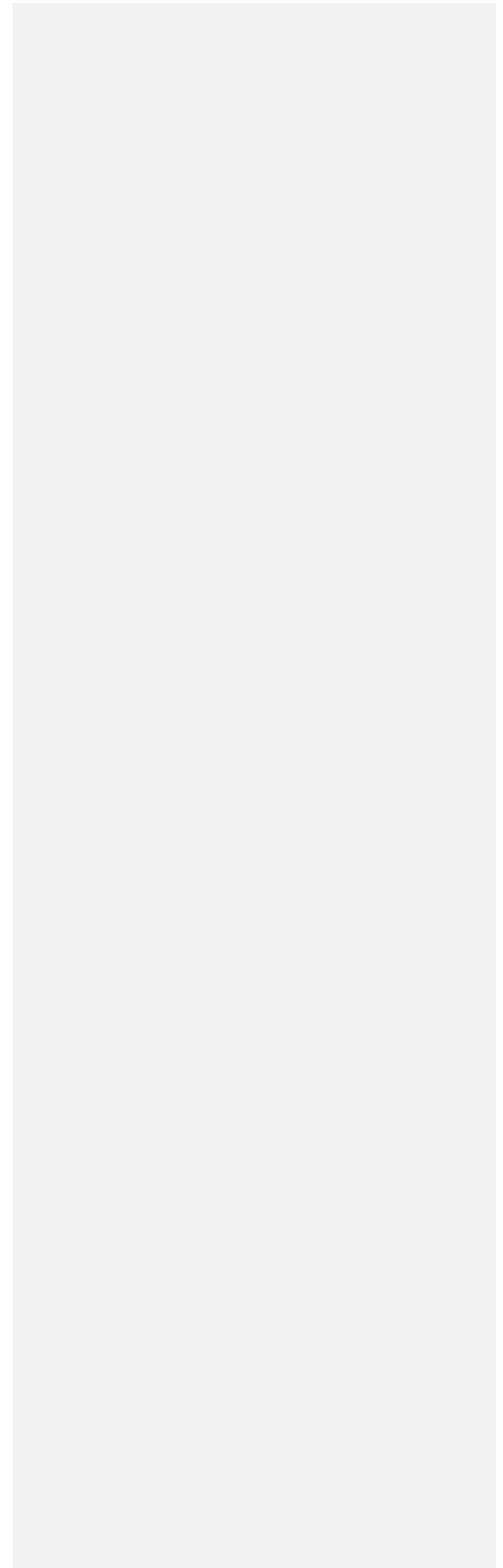
Mean Difference	± SD	± 1,16	± 0,79	± 0,82	± 3,82	± 0,79	± 3,21
	P-value	0,65	0,3	0,29	0,08	0,07	0,05

490
491
492
493
494
495
496
497
498
499
500
501
502

Figure legends

503
504
505
506
507
508
509
510
511
512

Fig. 1. 3D computation performed in a stereolithographic file obtained from a computed tomography reconstruction (CT aCAD) of a 2-years-old French Bouledog. After the 3D computation, femoral axes appear in the bone model (A). The green line is the femoral head and neck axis (FHNA), the blue lines represent the mechanical axis (MA) and the hip joint orientation line (HJOL), the red line is the proximal femoral long axis (PFLA) and the gold line is the transcondylar axis (TCA). (B) Cranial and caudal aspect of the proximal femoral epiphysis. Notice the fitting of the femoral head and the section of the femoral neck (light blue). (C) Medial-lateral



513 and caudal-cranial views of the femoral condyles. Note the sphere fitting of both condyles (light
514 blue spheres) as well as the green vertices that represent the contact area of the TCA.

515

516 Fig. 2. 3D computation performed in a stereolithographic file obtained from a 3D-scanner
517 acquisition (3D aCAD) of a 4-years-old Bernese mountain dog (A). The green line is the femoral
518 head and neck axis (FHNA), the blue lines represent the mechanical axis (MA) and the hip joint
519 orientation line (HJOL), the red line is the proximal femoral long axis (PFLA) and the gold line is
520 the transcondylar axis (TCA). (B) Cranial and caudal aspect of the proximal femoral epiphysis.
521 Notice the presence of red vertices outside of the femoral head fitting which represent parts of the
522 acetabulum excluded from the computation. (C) Medio-lateral and caudal-cranial aspects of the
523 distal femoral epiphysis. TCA, PFLA and MA are visible.

524

525 Fig. 3. Cranio-caudal views of four abnormal femurs after importation on Rhinoceros. (A) Right
526 femur of a 12-years-old German Shepherd severely affected by osteoarthritis (OA) of the femoral
527 head. (B) Right femur of a 10-years-old Pug which had a severe degeneration of the femoral head
528 and neck. (C and D) Left chondrodystrophic femurs affected by mild (C) and severe OA (D) of the
529 distal femoral epiphysis. The dogs were an 8-years-old French Bouledog and a 13 years-old
530 Dachshund.

531

532 Fig. 4. Graphical representation of the regression analysis. Line (A): regression
533 line of the totality of the femurs assessed for each angle. The R^2 are $>80\%$ for all three
534 angles. Line (B): regression analysis of group 1 (normal femurs). The R^2 are $>93\%$, having the
535 FTA measurement as the most accurate angle. Line (C): graphical representation of the
536 regression of group 2 (abnormal). The aLDFA angle was the most accurate ($R^2 > 93\%$), while the
537 FTA the most challenging to measure ($R^2 > 82\%$).

538

539 Fig. 5. Digital cranio-caudal photograph of the femur specimen of a 12-years-old German
540 Shepherd. (B and C) Cranial and caudal views of the femoral head and neck. The green line is the
541 femoral head and neck axis (FHNA), the blue lines represent the mechanical axis (MA) and the hip
542 joint orientation line (HJOL), the red line is the proximal femoral long axis (PFLA). Observe that
543 the osteophytes fall outside the green sphere and are not considered for fitting of the femoral head.
544 (D) Caudal view of the femoral condyles: the MA and transcondylar axis (gold line) are drawn. (E)
545 Femoral cranio-caudal view after the 3D computation.
546
547
548
549
550

